

Inclusion of the lesion of chronic stroke patients into a volume conduction model

Simulating the influence of the lesion on the electric field distribution generated by tDCS

F.E.M. Jeukens^{1,2*}, A. Schouten¹, M. Manoochehri¹, R. W. Selles², J. van der Crujisen², T. Oostendorp³, M. C. Piastra³

Abstract—Stroke is a cerebrovascular disorder with 15 million cases every year worldwide. The most common symptom is motor deficits. In order to overcome such symptoms, the motor brain either repairs the damaged tissue or reorganises to compensate for the injured brain region. To stimulate this reorganisation transcranial Direct Current Stimulation (tDCS) is considered to be a promising therapeutic intervention. Simulations of electric field distributions generated by tDCS currently entail individualised volume conduction models to improve tDCS. A volume conduction model includes geometry and conductivity properties of tissue types in healthy subjects. When applying existing models to chronic stroke subjects, electric field distribution patterns differ substantially compared to healthy subject distribution patterns. In current models, the lesion is not identified and acknowledged as a distinctive tissue type, as it is yet unclear what the lesion influence is. However, the lesion is a potential source of variability in desired electric field distribution which could result in different motor recovery. A volume conduction model is designed by combining the software SimNIBS, which can segment the head of healthy subjects and LINDA, able to distinguish lesion tissue of chronic stroke subjects. The location and the conductivity value of the lesion seem to influence the electric field distribution of tDCS where this individualised model is preferred. Including the lesion is an important advance towards the use of volume conduction models for chronic stroke subjects to prospectively find optimal electrode configurations, keep the safety margins and to prospectively analyse the results of tDCS.

Index Terms—tDCS, volume conduction model, lesion, stroke, conductivity, motor rehabilitation, simulation, LINDA, SimNIBS

¹ Department Biomechanical Engineering, Delft University of Technology, Delft, The Netherlands

² Department of Rehabilitation Medicine, Erasmus University Medical Center, Rotterdam, The Netherlands

³ Cognitive Neuroscience, Donders Institute for Brain, Cognition and Behaviour, Radboud University Nijmegen Medical Centre, Nijmegen, The Netherlands

* **Corresponding author:** Studentnumber: 4256980

I. INTRODUCTION

STROKE is the leading cause of adult long-term disability worldwide. One out of six people suffers from a stroke, according to the World Health Organization [1]. Stroke is a cerebrovascular disorder where the blood flow in the brain is interrupted, either by occlusion or rupture of a blood vessel. A deficit of oxygen is caused in a certain brain area, the tissue will be damaged, and this area is called the lesion. A lesion leads to dysfunction through the interruption of structural and functional pathways, and deregulation of cortical excitability and the motor cortex can be damaged or replaced by lesion tissue[2]. 80% of stroke survivors encounter motor impairments resulting

from brain damage, which makes it one of the main challenges[3]. The quality of life of patients is affected by difficulties in performing daily activities and social participation [4].

In the first months post stroke, patients often regain between 40% and 70% of the initial clinical deficit. Clinical progress is caused by brain-recovery mechanisms occurring spontaneously already in the first days to weeks post stroke [5][6] [7]. Neuroplasticity is the basis of this mechanism [8] which is defined as the ability of the brain to change continuously throughout an individual's life, e.g., brain activity associated with a given function can be transferred to a different location, the proportion of grey matter can change, and synapses may strengthen or weaken over time. Through neuroplasticity, the neural networks will be optimised after a brain injury[9]. The clinical recovery where body functions are restored can be caused by restitution and substitution, where restitution is the repair of damaged tissue and substitution the reorganisation of neural pathways when other brain areas compensate for the damaged tissue to regain motor function [10].

Substitution is enabled by the diffuse and redundant connectivity existing in the brain [11]. Functional changes and circuits in non-injured regions can intervene in supporting compensatory mechanisms and in this way, reorganisation is related to the recovery of motor function [7][6]. Stroke lesions lead to different reorganisations; efficient information processing critically deviates, reduction of within-hemisphere segregation between different brain systems and the connectivity is changed between both hemispheres, resulting in contralesional activity by motor outcome produced by the ipsilesional hemisphere[5] [12].

Transcranial Direct Current Stimulation (tDCS) is one of the therapeutic interventions to stimulate reorganisation of the motor brain, to overcome motor impairments and stimulate recovery. TDCS is a promising non-invasive brain stimulation technique in research state and a viable tool due to its limited side-effects, safety, availability, costs, portability and relatively simple use[2]. Target and reference electrode are placed on the scalp. A low-intensity direct current, between 0.5 and 2 mA, is delivered and conducted by the brain tissues to complete the circuit. Cortical regions exposed to higher electric field strength are more likely to modulate, which enhance motor recovery [13]. To stimulate motor recovery, the target area is the motor cortex, and the electric field strength should be as high as possible in that area.

The electric field distribution of tDCS depends on various factors: the size, polarity, amount and position of the electrodes, the applied current intensity and the

properties, as conductivity, of the tissue in the stimulated area[2][14][15]. To investigate the effect of different settings of these parameters and to predict if the current will reach the target area, it is possible to simulate the electric field distribution through a so-called volume conduction model.

Requirements of a volume conduction model are the geometry of the structures in the head and their conductivity values. Such software is Simulation of Non-invasive Brain Stimulation (SimNIBS) where firstly a magnetic resonance image (MRI) of the head is converted into high-quality tetrahedral volume meshes. Then the volume meshes are used in the electric field with calculations based on finite elements. The result is a visualisation of the electric field distribution of the simulated tDCS stimulation and based on the outcome of the electric field distribution. The electrode configuration can be determined to reach the motor cortex.

Nowadays, for the simulation of the electric field distribution generated by tDCS, volume conduction models of healthy subjects are used. A volume conduction model of the head is created which includes the geometry and conductivity of scalp, skull (compact bone and spongy bone), grey matter (GM), white matter (WM) and cerebrospinal fluid (CSF).

Various clinical tDCS studies where motor excitability have been modulated in stroke patients show different results wherein some studies 50% of stroke patients fail to show a response to stimulation [2]. The different outcomes of studies could be caused by the use of inaccurate volume conduction models not representing the brain of chronic stroke subjects. The volume conduction models used for healthy subject gives different results for stroke subjects which could be caused by the lesion[16]. Because lesions can present conductivity values dramatically different then is assigned by existing tools. Incorrect conductive properties can be introduced in the volume conduction head model[17] and will finally lead to inaccurate electric field distribution while simulating tDCS[13]. They are resulting in either undesired electric field strength values in the target area or unsafe high values. The influence of the lesion is not clear though a potential source of variability in desired electric field distribution which could result in different motor recovery.

This study aims to develop an automatic pipeline to investigate the influence of a lesion on the simulated electric field distribution in volume conduction head models of chronic stroke subjects. This simulation study will quantify the relation between lesion conductivity and the electric field distribution for chronic stroke subjects compared to simulation models where the lesion is not included.

In this study, a volume conduction head model is created by segmenting the head into the scalp, skull (compact bone and spongy bone), GM, WM and CSF. The lesion will be included in the volume conduction head model by relabeling the tissues on the location of the lesion. After that, tDCS is simulated with the model where the lesion is not included and with the model where the lesion is included and assigned different values for conductivity. Finally, the method will be evaluated for one chronic stroke subject by comparing the electric field distribution

in the two models.

II. METHODS

First, the automatic generation of the volume conduction model is described. The tDCS simulation settings are presented, and finally, the two different head models and the measures for the quantification of the differences for the whole grey matter volume and within the target area are introduced to analyse the results of ipsilesional and contralesional stimulation of 1 chronic stroke subject.

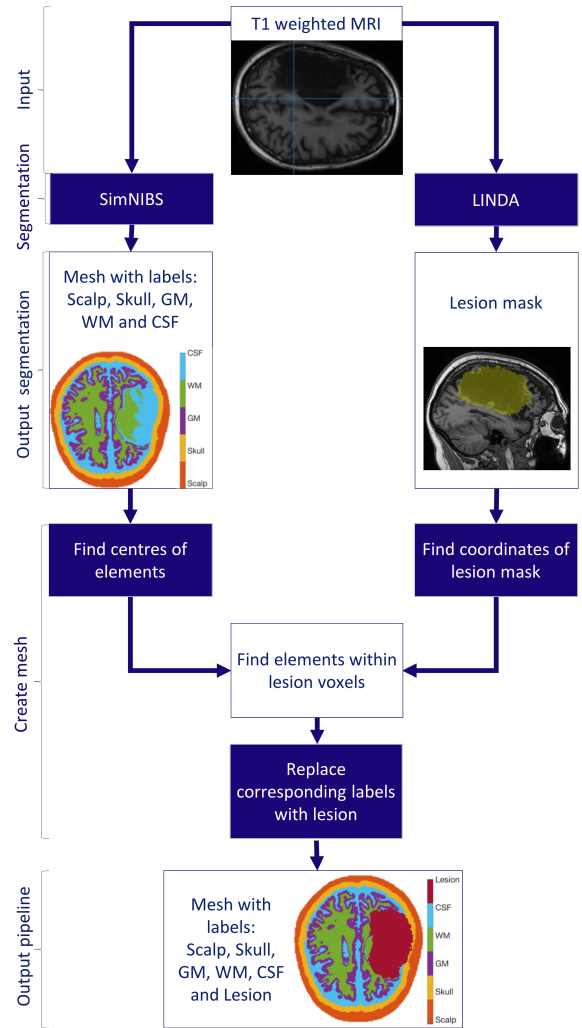


Fig. 1. Automatic pipeline to create volume conduction model of a chronic stroke subject where the lesion is included in the model. The input is a T1w, SimNIBS segments the head into the scalp, skull (both compact and spongy bone), GM, WM and CSF. LINDA identifies the lesion and the corresponding SimNIBS elements are relabelled into lesion.

A. Volume conduction model

The first step to create a volume conduction model is to assign each voxel of the T1 weighted MRI (T1w) to a specific tissue class. On the one hand, the segmentation of the T1w into the scalp, spongy bone and compact bone of the skull (compact bone and spongy bone), GM, WM and CSF was performed with the SimNIBS software version 2.1.2 (2019)[18]. Only SimNIBS is not able to recognise lesion tissue. So, on the other hand, the

software named Lesion Identification with Neighborhood Data Analysis (LINDA) version 0.5.0 is needed to identify the stroke lesion[19]. Finally, the two segmentation tools were combined in order to create a volume conduction model representing the brain of a chronic stroke subject. The Matlab-based automatic pipeline of the process to create the desired model is visualised in Figure 1 and described in the following.

1) *MRI settings*: The input of the automatic pipeline is a T1w of a chronic stroke subject, where chronic is defined as more than six months post stroke onset. Here the T1w was acquired with the following settings: TR = 8100 ms, TE = 100 ms, flip angle = 90 degrees, FOV = 240 x 240 x 130 mm, voxel size = 2.5 x 2.5 x 2.5mm and with fat suppression.

The T1w should be acquired with a fat suppression method, so not using a low readout bandwidth. Because then the positions of the (fatty) spongy bone and subcutaneous fat will not be displaced in the T1w due to the chemical shift artefact and the segmentation of the GM pial surface and the boundary between CSF will be more accurate, because the spongy bone will not touch the GM[20].

2) *Segmentation whole head*: The T1w accounted as the input of SimNIBS to reconstruct the realistic geometries of Scalp, Compact bone, Spongy bone, GM, WM and CSF. SimNIBS is a fast and free software on www.SimNIBS.org. The toolbox of SPM12 is used to segment the T1w and performs more accurate compared to other segmentation tools, especially on the segmentation of the skull[20]. The accuracy of the segmentation of the head models has a strong influence on the accuracy of the calculated electric field distributions of the tDCS simulation[21]. In particular, the segment of the skull exerts a strong influence on the electric field distribution due to the much lower conductivity compared to the other tissues. SimNIBS offers headreco as an option for the segmentation. The SPM12 toolbox is used and provides the computational anatomy toolbox CAT12, which creates surface reconstructions of the GM[22]. SimNIBS is not able to recognise the lesion as a separated segment and will assign the lesion part of the brain in one of the geometries.

3) *Segmentation lesion*: Currently, the gold standard to segment a lesion is the manual procedure where the voxels belonging to the lesion are assigned manually per slice. An expert is necessary with expertise in neuroanatomy and manually segmenting is time-consuming and labour-intensive. The results could be inconsistent from rater to rater. For large-scale stroke rehabilitation neuroimaging analyses the manual procedure is not feasible. In this study, the fully automated software of LINDA was used. It is a supervised (based on machine learning), mono channel algorithm trained on over 100 patients cross-institutional to segment left-hemispheric chronic stroke lesions from T1w[19]. T1w of right-sided lesions were first flipped before using LINDA. The output was the mask of the lesion tissue as a nifti file.

4) *Creating a mesh*: The software SimNIBS creates a tetrahedral volume mesh based on the segmented T1w, i.e., the output of step 2. The mesh, therefore, does not contain the lesion. To create a mesh which is more

representative for the chronic stroke subject, the lesion segmented by LINDA was included. In order to do so, first, the coordinates of the lesion mask voxels were identified. Then the centres of the mesh elements within the lesion mask voxels were therefore labelled as "lesion".

B. tDCS simulation

In order to investigate the influence of the lesion conductivity on the volume conduction model, different values were applied during different tDCS simulations. They were applied with the same software as the segmentation: SimNIBS. First, the electrodes were built into the model and calculations were performed to determine the effects.

1) *Electrode configuration*: Two tDCS electrodes were modelled as elliptical patches with a size of 1 cm x 1 cm and thickness of 3 mm. To simulate stimulation of the left and right motor cortex, the electrodes were placed at the C3 and the Fp2 and the C4 and the Fp1, respectively, as shown in Figure II-B1 [23]. The electrodes are modelled as additional volumes on top of the skin. The nodes of the mesh closest to the anode were assigned with a potential of $+\Phi$ and to the cathode with $-\Phi$, where a total current of 2.00 mA was simulated.

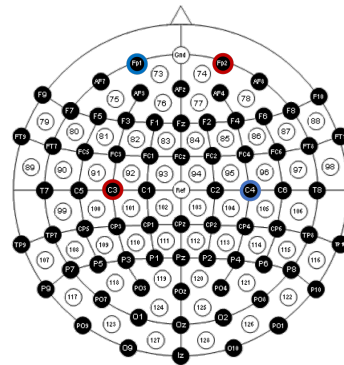


Fig. 2. The electrode positions to stimulate the left motor cortex are C3 and Fp2, depicted in red and to stimulate the right motor cortex the positions are C4 and Fp1, depicted in blue using a 10/20 EEG system[23]

2) *Conductivity values*: The conductivity values for the healthy tissues were obtained from the SimNIBS software and the model was simulated for 11 lesion conductivity values ranging from 0.50 till 2.00 S/m[17][24]. All conductivity values are presented in Table I.

3) *Calculations*: The potential Φ [V] was computed at each node of the mesh with the software SimNIBS. By solving numerically with the finite element method (FEM) it allows one to break down structures into smaller triangle and tetrahedral elements, which the FEM mesh is made of. By assigning distinct electrical properties to the individual elements, the following Laplace equation can be fully solved:

$$\nabla \cdot (\sigma \nabla \Phi) = 0 \text{ in } \Omega,$$

where σ is the conductivity value [S/m] and Ω the head model. As a further computation, the electric field $E = -\nabla \Phi$ was computed in each element of the mesh.

TABLE I
CONDUCTIVITY VALUES TDCS SIMULATION

Tissue	Conductivity [S/m]
Scalp	0.465
Skull:	
<i>Compact bone</i>	0.008
<i>Spongy bone</i>	0.025
GM	0.275
WM	0.126
CSF	1.654
Lesion	0.50, 0.65, 0.80, 0.95, 1.10 1.25, 1.40, 1.55, 1.70, 1.85, 2.00

Presented are the conductivity values assigned to 7 tissues types in the volume conduction model. With the conductivity values tDCS was simulated. For the lesion the model was evaluated with 11 different conductivity values.

C. Analysis

In order to investigate the influence of the conductive properties of the lesion on tDCS simulation of the motor cortex, two volume conduction models were created.

- **Model 1** where the lesion is not included, and the lesion voxels of the T1w were assigned to, scalp, skull (compact bone and spongy bone), GM, WM or CSF according to SimNIBS.
- **Model 2** was created according to the method described above where the geometry of the lesion is included as well as the conductive properties.

The distribution of the electric field was investigated for the two volume conduction models and repeated with 11 different conductivity values assigned to the lesion (see Table I). They were compared: 1) in the whole GM volume and 2) within a target area, the motor cortex and for Model 2 within the lesion.

1) *Whole grey matter volume* : The electric field strength trough the whole GM volume is analysed for Model 1 and 2. The maximum values for the electric field strength are compared between the two models.

2) *Target area*: To investigate the difference of the tDCS simulation exactly in the target region within the GM, a small volume was constructed. A medical doctor visually identified the motor hotspot, and a sphere with a radius of 1 cm around the hotspot was selected as the region of interest which contained all elements within this volume of GM. To estimate the effect of the different conductivity values, the mean and maximum of the electric field strength within the sphere were used. The values were compared between Model 1 and Model 2. Also, the mean and maximum electric field strength were calculated of the lesion segment for every conductivity value in Model 2.

III. RESULTS

First, the general results are presented concerning the automatic pipeline. The volume conduction model created by SimNIBS contained 3,536,411 tetrahedral elements in total. 176,734 were relabelled into lesion because their centres were located within the 208,312 voxels, which were segmented as lesion according to LINDA as presented in Table II. The lesion volume was 183,09 ml. Furthermore, the outcomes of the automatic pipeline are

shown on two different levels: Firstly, the results for the electric field for the whole grey matter volume and secondly, for the target regions one representing the motor area for the hand and the other the lesion.

TABLE II
AMOUNT OF ELEMENTS OF THE VOLUME CONDUCTION MODEL

	Total	Lesion	MC (i)	MC (c)
Tetrahedra	3,536,411	176,734	108	2293
Triangles	827,832	36,364	50	663

MC (i) is the ipsilesional motor cortex, MC (c) the contralesional.

The electric field strength magnitude injected in the grey matter by 2 mA tDCS simulated with Model 2 ranged from 0.017 till 1.13 V/m for ipsilesional stimulation and from 0.004 till 0.90 V/m for contralesional stimulation.

A. Whole grey matter volume

In Figure 3 is the electric field distribution presented through the whole GM volume. For ipsilesional stimulation, the maximum electric field strength in Model 1 (without lesion) was 2.06 V/m. For Model 2 (where the lesion was included) this value increased from 1.04 till 1.13 V/m respectively for lesion conductivity values between 0.50 and 2.00. A decrease in electric field strength through the whole GM volume between the two models was observed between 49.42% and 45.25%.

For contralesional stimulation, the maximum electric field strength was 1.31V/m in Model 1 and decreases were observed of 38.43% till 34.65% for this value in Model 2 with lesion conductivity of 0.50 till 2.00 S/m respectively as presented in Table III. The maximum values differed in location between Model 1 and 2 but stayed the same for all lesion conductivity values.

TABLE III
MAXIMUM ELECTRIC FIELD STRENGTH IN GM WHEN SIMULATING 2MA TDCS

	σ_l	E_{mx}^I	E_{mx}^C
	[S/m]	[V/m]	[V/m]
Model 1	-	2.06	1.31
Model 2	0.50	1.04	0.81
	0.65	1.06	0.85
	0.80	1.08	0.88
	0.95	1.10	0.89
	1.10	1.10	0.90
	1.25	1.11	0.90
	1.40	1.11	0.89
	1.55	1.12	0.89
	1.70	1.12	0.88
	1.85	1.13	0.87
	2.00	1.13	0.86

From left to right: Conductivity value assigned to lesion (σ_l), Maximum electric field strength in GM by stimulating the ipsilesional motor cortex (E_{mx}^I), Maximum electric field strength in GM by stimulating the contralesional motor cortex (E_{mx}^C).

B. Target area

The target area for the stimulation of the ipsilesional and contralesional motor area for the hand is shown in Figure

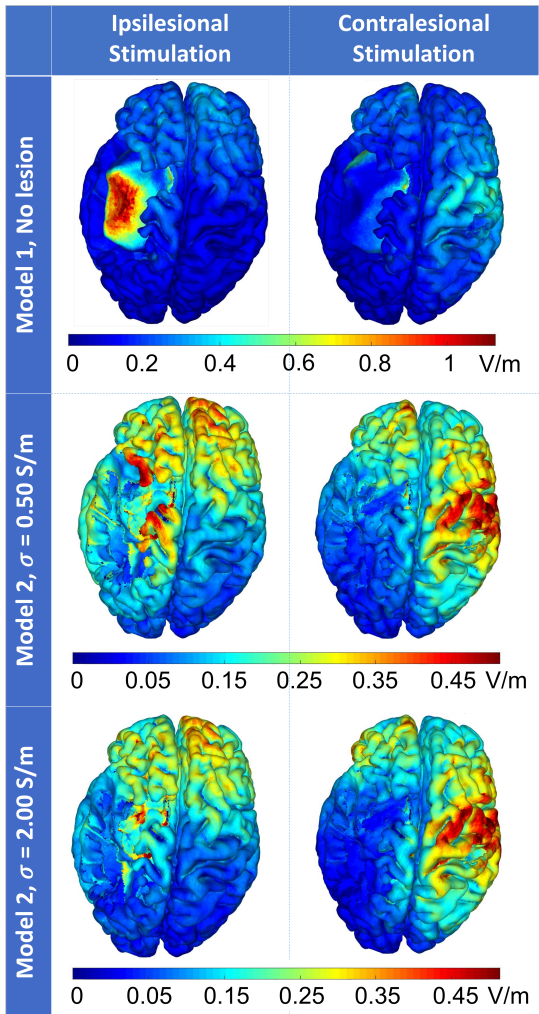


Fig. 3. The Electric field distribution in V/m in the whole grey matter volume. Generated by 2mA tDCS simulation for ipsilesional and contralesional stimulation. In model 1 no lesion was included in the volume conduction model and for model 2 the lesion was included with a conductivity of 0.50 and 2.00 S/m.

4. The left motor area for the hand (ipsilesional side) consisted of 108 tetrahedral and 663 triangle elements and was stimulated by electrodes positioned at C3 and the Fp2. Simulated with Model 2 the mean electric field strength in this area was 0.43 V/m where the lesion conductivity was 0.5 S/m and the higher the lesion conductivity, the lower the mean electric field strength became till 0.27 V/m for a lesion conductivity of 2.00 S/m. The values simulated with Model 2 were compared to Model 1 and were always higher, for a lesion conductivity of 0.50 S/m the electric field strength was 63.1% more in Model 2. The higher the lesion conductivity, the lower the mean electric field strength was in Model 2, as presented in Figure 5 till 1.7% for a lesion conductivity of 2.0 S/m. With the electrodes positioned at C4 and the Fp1, the right (contralesional) motor cortex was stimulated. This target area contained 2293 tetrahedral and 36364 triangle elements and the mean electric field strength was for every lesion conductivity similar. For contralesional stimulation, the mean electric field strength in the contralesional motor cortex was 0.30V/m and the differences between Model 1 and Model 2 were also minimal with a maximum

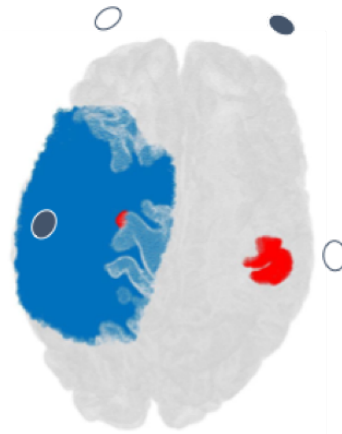


Fig. 4. Visualization of the GM and the target areas, in red the left and right motor area for the hand and in blue the lesion. With white and black are the positions of the electrodes shown for respectively ipsilesional and contralesional stimulation.

difference of 1.38% as shown in Figure 5.

IV. DISCUSSION

In this study, a volume conduction model is introduced containing the geometry of the structures and the conductivity values of the scalp, skull (compact bone and spongy bone), GM, WM, CSF and the lesion for a chronic stroke subject. An automatic pipeline is presented to create individualised head models to simulate tDCS, which is a desired step in the research field of improving motor recovery by tDCS.

In the first place, the developed volume conduction model could provide an individualised electrode configuration for chronic stroke subjects. In other words, it means that the volume conduction model is useful in the simulation of tDCS, which consists of modelling the pathway of the current through the head between the anode and the cathode for a specific electrode configuration especially for chronic stroke subjects. The electric field distribution and the location of the highest electric field strength, where the electric field strength is the highest, where reorganisation of the grey matter is most likely[13], is dependent on the electrode configuration and. Recent studies did not make use of individualised volume conduction models for chronic stroke subjects to find the optimal configuration of the electrodes. The outcomes of recent studies are no effects of motor recovery after tDCS compared to sham tDCS for chronic stroke subjects[25]. Also, a systematic review of Elsner et al. (2017)[26] presented, based on sixteen clinical trials including 302 participants in total, no evidence for the effect of different tDCS types on the upper limb motor function of chronic stroke subjects. However, for 12 randomised controlled trials with 284 participants, the effect of tDCS on activities of daily living capacity gave moderate effects[26]. When tDCS was combined with training of a specific task, the stimulation had a positive effect on the specific task. However, no evidence was found of a generalised effect on the motor recovery[27]. From this can be concluded that tDCS could have a positive effect on the motor recovery of chronic stroke subjects and could be a promising therapeutic

intervention, but improvements are necessary. Because the literature does not provide clear guidelines regarding the applied current intensity, tDCS type or electrode configuration [28], a reliable model of the head of chronic stroke subjects could help decide which individualised electrode configuration should be applied. Secondly, the presented volume conduction model could provide insight why clinical tDCS studies show different results for chronic stroke subjects. For complex phenomena such as motor recovery knowledge, not only the electric field strength in the target area and thus the corresponding electrode configuration is critical, but also the resulting electric field distribution. Because brain regions do not operate in isolation but interact with other regions through networks. As such, stimulation of one region may impact and be impacted by other regions in its network[29]. With the volume conduction model, presented in this study, tDCS can be simulated with the applied electrode configuration, and more insight can be given about the reason for the effectiveness. Because fundamental unknowns remain about both the motor recovery after stroke and the neurophysiology of tDCS.

Thirdly, an automatic pipeline to create individualised head models to simulate tDCS is a desired step in the research field of improving motor recovery because research is accelerated and could easily be extended. In previous studies, the geometry of the lesion was assigned manually, a subjective procedure which could differ from rater to rater. In contrast with existing volume conduction models, the pipeline presented in this study presents a fully automatic inclusion of the lesion, which is objective and less time-consuming. The automatic pipeline provides to include many chronic stroke subjects in a more accurate tDCS study. The input of the pipeline is only a single T1w, which decreases the burden on stroke patients, because of little acquisition time. Next to this, the acquisition costs are lower, and the chances of motion-related artefacts are decreased.

Finally, the volume conduction model in this study contains the geometry and the corresponding conductivity values for the scalp, skull (compact bone and spongy bone), GM, WM, CSF and lesion, the methodology also lends itself to be useful for other purposes beside tDCS simulation, such as transcranial magnetic stimulation (TMS) simulations and EEG source localisation.

In short, the developed automatic pipeline in this study is suited to model the effect of the lesion automatically on the electric field distribution in a chronic stroke subject for a range of conductivity values between 0.50 and 2.00 S/m. The next two sections provide a discussion about the achieved results on the level of the whole GM volume and on the target area, which is the motor cortex.

A. Whole grey matter volume

Not only the electric field distribution in the target area is of importance, but also the electric field distribution in the remaining GM is essential to study. Firstly, to be able to understand the motor recovery after stroke and the neurophysiology of tDCS and secondly the range of the electric field strength can be investigated to see if safety margins have remained.

The safety of tDCS is dependent on levels of current density and intensity, electrode size and electrode locations. If the established safety guidelines are followed compiled by Fertonani et al. (2015) [30] the electric field strength will not exceed the safety limits in the GM for healthy subjects. In a previous study of Minjoli et al. (2017) [16] the safety was examined for stroke subjects when tDCS was simulated on the volume conduction model created by SimNIBS, where the lesion was not included. The model used by Minjoli et al. [16] is comparable to Model 1 presented in this study and gave in most of the GM decreased electric field strength compared to the healthy control. The maximum electric field strength was not substantially different between the head models with the lesions and healthy control. In this study, the maximum electric field strength simulated with Model 2 was even lower compared to Model 1 taking the same safety guidelines into account of Fertonani et al.[30]. So it seems that a lesion with a conductivity value between 0.50 and 2.00 S/m does not have a negative influence on the safety of tDCS for both stimulation configurations and the maximum electric field strength falls within the safety limits.

For both stimulation configurations and all lesion conductivity values, the maximum electric field strength is lower simulated with Model 2 compared to Model 1. The overall electric field strength is also lower in Model 2 compared to Model 1 for ipsilesional stimulation, as presented in 3. The values of the electric field strength can be compared with the study of Minjoli et al. (2017) [16] where for healthy subjects and stroke subjects tDCS was simulated with a volume conduction model created with the same procedure as Model 1. A substantial reduction ($\approx 30\%$) of the average field strength for the stroke subjects simulated with the same procedure as Model 1 at almost all distances to the electrode were observed[16]. In another study healthy subjects were compared with stroke subjects where the lesion was manually included with a conductivity value of 1.675 S/m, so for stroke subjects, a model was created comparable to Model 2 [31]. An increase of the electric field strength is observed for Model 2 compared to healthy subjects [31]. When the healthy subjects are taken as the baseline, Minjoli et al. found a decrease compared to their Model 1 and Wagner et al. an increase compared to their Model 2. The increase in the Model 2 of Wagner et al. compared to the decrease in electric field strength of Minjoli et al. is not in line with the overall decrease found in Model 2 compared to Model 1 presented in this study. However, comparing the electric field strength with other studies is complicated because the value is dependent on the specific geometry of the subject, the lesion location and the electrode configuration.

For both stimulation protocols, the maximum electric field strength is lower in Model 2 compared to Model 1, which could confirm the observations of Datta et al. (2011)[13], that the lesion has a preferred pathway for the current, resulting in an altered electric field distribution and lower strength in the grey matter. For contralesional stimulation, the difference between the two models is smaller. When the lesion is located far away from the electrodes, the influence on the electric field distribution

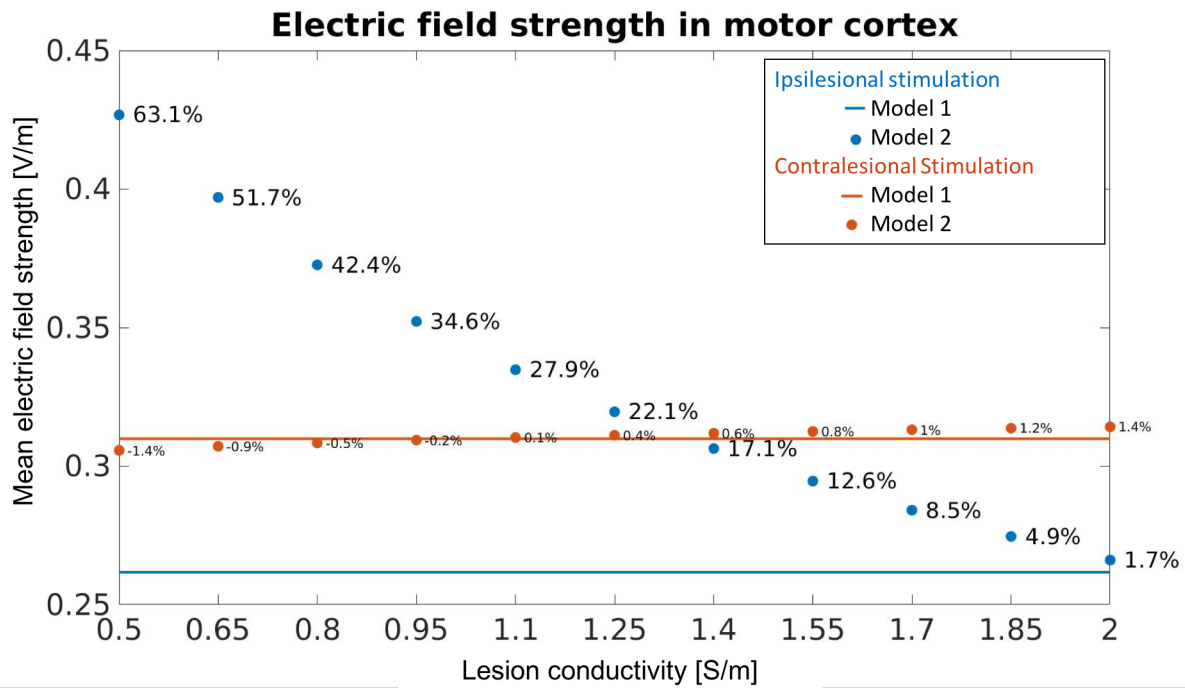


Fig. 5. In blue, the mean electric field strength through the motor cortex for ipsilesional stimulation is presented and in red for contralesional stimulation. The difference between Model 1 and Model 2 of the mean electric field strength in the motor cortex are presented in percentages.

is limited, from which can be deduced that the influence of the lesion is dependent on the location.

B. Target area

The investigation of the electric field strength in the target area is important because tDCS is the most effective for motor recovery when the higher electric field strength is present in the target area[13]. To investigate the effect of tDCS simulation in a specific target region within the GM, a small volume was constructed representing the motor cortex. A medical doctor assigned the centre of the target area. For the contralesional hemisphere, this process gave a reliable set of elements. However, for the ipsilesional hemisphere, only a few elements in the area of the motor cortex were available for analysis due to the geometry of the lesion. By the observation can be deduced that the location of the lesion in the volume conduction model might provide a good indication for the remaining target area available for stimulation. An example would be to preferably stimulate the contralesional motor cortex to promote reorganisation of the motor brain.

Though the ipsilesional target area is a small region consisting only of a few elements which could influence the outcomes, a striking result is found for ipsilesional stimulation. For every lesion conductivity value, the mean electric field strength simulated with Model 2 where the lesion is included is always higher and never crossing the value simulated with Model 1. In principle is expected that the outcomes of the mean electric field strength simulated by Model 2 would be the same at a certain point as Model 1 when the conductivity value of the lesion area simulated in Model 2 is comparable to Model 1. However, it is not straight forward to compare Model 1 to Model 2 because the lesion tissue in both models varies; in

Model 1 the lesion tissue consists of a heterogeneous mix of GM, WM and CSF, whereas in Model 2 the lesion tissue is homogeneously characterised by a single conductivity value. Also, for ipsilesional stimulation is the mean electric field strength decreasing by an increasing lesion conductivity simulated by Model 2, as shown in Figure 5. In general, a high conductivity value for the lesion provides a path of low resistance, which results in an accumulation of current in the lesion. If in addition to this, the lesion has a comfortable geometry concerning the target area, the current will be accumulated in the target area.

For contralesional, the lesion does not have a significant influence on the mean electric field strength in the motor cortex, indicating the influence of the lesion to be location dependent.

For both the ipsilesional and contralesional stimulation for this specific stroke subject, the maximum electric field strength is outside the target area, which confirms the need to develop a volume conduction model that includes the lesion to be able to find an electrode configuration which generates a maximum in the desired area. Moreover, general guidelines of the electrode configuration to reach the motor cortex could be revised based on this model[28] and are necessary because as mentioned previously, the goal of tDCS is to generate the maximum electric field strength within the target area to be the most effective.

C. Limitations and recommendations

Some limitations of the current study can account for future research. First, to conclude what the exact influence is of the lesion on the electric field distribution, the

lesion conductivity should be determined. In current tDCS simulation studies, lesion tissue regions are manually appointed in order to simulate the electric field density distributions in the brain. Generally, a lesion conductivity of 1.675 S/m, which corresponds to the conductivity value of CSF, is appointed to the lesion tissue regions[13][31]. Regarding 1.675 S/m as a realistic value and adequate lesion conductivity level, previous research resulted in a maximum difference of 21% for the electric field distributions, compared to healthy subjects[16]. Based on this result, it can be concluded that the lesion conductivity is an important factor to take into account during modelling and should be determined. Secondly, in this study, the lesion is considered as a homogeneous tissue with one conductivity value for the whole lesion. However, lesion tissue could be heterogeneous and could exist for a significant part of CSF. Assigning the CSF part of the lesion could give a more realistic model. So, realistic lesion conductivity levels might neither be in the vicinity of the conductivity level of CSF nor uniform[17]. Another limitation is that the mesh of the head was constructed before including the lesion. The area could be described by a rough mesh, which could lead to an inaccurate description of the lesion because with big or small elements. Furthermore recommended is to test the automatic pipeline on more than one subject.

V. CONCLUSION

With the inclusion of the lesion in the volume conduction head model, an automatic pipeline is developed to investigate the influence of the lesion on the electric field distribution of tDCS simulation. From the results of this simulation study, the following can be concluded:

- With the inclusion of the lesion in the volume conduction head model, an automatic pipeline is developed which shows an influence of the lesion on the electric field distribution of tDCS simulation.
- The influence of the lesion on the electric field distribution is dependent on the location of the lesion. With tDCS simulation of the ipsilesional motor cortex, the lesion has more influence compared to contralesional stimulation.
- The influence of the lesion is dependent on its conductivity properties. In this particular subject, the more conductive the lesion tissue, the less influence on the electric field distribution in the motor cortex compared to the volume conduction model where the lesion is not included.

The results give new insights on how to develop a volume conduction model of chronic stroke subjects used for tDCS simulation and suggest room for improvement in the outcomes and applications of the therapeutic intervention. Important advancement could be made toward the use of volume conduction models for chronic stroke subjects to prospectively find optimal electrode configurations and to prospectively analyse the results of tDCS.

REFERENCES

- [1] Judith McKay, George A Mensah, Kurt Greenlund, and Shanthi Mendis. *The atlas of heart disease and stroke*. World Health Organization, 2004.
- [2] Stephanie Lefebvre and Sook-Lei Liew. Anatomical parameters of tDCS to modulate the motor system after stroke: a review. *Frontiers in Neurology*, 8:29, 2017.
- [3] Gert Kwakkel, Janne M Veerbeek, Erwin EH van Wegen, and Steven L Wolf. Constraint-induced movement therapy after stroke. *The Lancet Neurology*, 14(2):224–234, 2015.
- [4] Jodi D Edwards, Mieke Koehoorn, Lara A Boyd, and Adrian R Levy. Is health-related quality of life improving after stroke? a comparison of health utilities indices among Canadians with stroke between 1996 and 2005. *Stroke*, 41(5):996–1000, 2010.
- [5] Joshua S Siegel, Benjamin A Seitzman, Lenny E Ramsey, Mario Ortega, Evan M Gordon, Nico UF Dosenbach, Steven E Petersen, Gordon L Shulman, and Maurizio Corbetta. Re-emergence of modular brain networks in stroke recovery. *Cortex*, 101:44–59, 2018.
- [6] Fabrizio De Vico Fallani, Silvia Clausi, Maria Leggio, Mario Chavez, Miguel Valencia, Anton Giulio Maglione, Fabio Babiloni, Febo Cincotti, Donatella Mattia, and Marco Molinari. Interhemispheric connectivity characterizes cortical reorganization in motor-related networks after cerebellar lesions. *The Cerebellum*, 16(2):358–375, 2017.
- [7] Sara Regina Meira Almeida, Jessica Vicentini, Leonardo Bonilha, Brunno M De Campos, Raphael F Casseb, and Li Li Min. Brain connectivity and functional recovery in patients with ischemic stroke. *Journal of Neuroimaging*, 27(1):65–70, 2017.
- [8] Tanja CW Nijboer, Floor E Buma, Caroline Winters, Mariska J Vansteensel, Gert Kwakkel, Nick F Ramsey, and Mathijs Raemaekers. No changes in functional connectivity during motor recovery beyond 5 weeks after stroke; a longitudinal resting-state fmri study. *PloS one*, 12(6):e0178017, 2017.
- [9] Guillaume Herbet, Maxime Maheu, Emanuele Costi, Gilles Lafargue, and Hugues Duffau. Mapping neuroplastic potential in brain-damaged patients. *Brain*, 139(3):829–844, 02 2016. ISSN 0006-8950. doi: 10.1093/brain/awv394. URL <https://doi.org/10.1093/brain/awv394>.
- [10] Michael Selzer, Stephanie Clarke, Leonardo Cohen, Gert Kwakkel, and Robert Miller. *Textbook of Neural Repair and Rehabilitation: Volume 1, Neural Repair and Plasticity*. Cambridge University Press, 2014.
- [11] Timothy H Murphy and Dale Corbett. Plasticity during stroke recovery: from synapse to behaviour. *Nature reviews neuroscience*, 10(12):861, 2009.
- [12] Jungsoo Lee, Eunhee Park, Ahee Lee, Won Hyuk Chang, Dae-Shik Kim, and Yun-Hee Kim. Alteration and role of interhemispheric and intrahemispheric connectivity in motor network after stroke. *Brain topography*, 31(4):708–719, 2018.
- [13] Abhishek Datta. Inter-individual variation during transcranial direct current stimulation and normalization of dose using mri-derived computational models. *Frontiers in psychiatry*, 3:91, 2012.
- [14] WOLNEI CAUMO, Izabel CC Souza, Iraci LS Torres, Liciane Medeiros, Andressa Souza, Alicia

- Deitos, Liliane Vidor, Felipe Fregni, and Magdalena Sarah Volz. Neurobiological effects of transcranial direct current stimulation: a review. *Frontiers in psychiatry*, 3:110, 2012.
- [15] Hayley Thair, Amy L Holloway, Roger Newport, and Alastair D Smith. Transcranial direct current stimulation (tdcs): a beginner’s guide for design and implementation. *Frontiers in neuroscience*, 11:641, 2017.
- [16] Sena Minjoli, Guilherme B Saturnino, Jakob Udby Blicher, Charlotte J Stagg, Hartwig R Siebner, André Antunes, and Axel Thielscher. The impact of large structural brain changes in chronic stroke patients on the electric field caused by transcranial brain stimulation. *NeuroImage: Clinical*, 15:106–117, 2017.
- [17] Federica Vatta, Paolo Bruno, and Paolo Inchingolo. Improving lesion conductivity estimate by means of eeg source localization sensitivity to model parameter. *Journal of Clinical Neurophysiology*, 19(1):1–15, 2002.
- [18] Axel Thielscher, Andre Antunes, and Guilherme B Saturnino. Field modeling for transcranial magnetic stimulation: a useful tool to understand the physiological effects of tms? In *2015 37th annual international conference of the IEEE engineering in medicine and biology society (EMBC)*, pages 222–225. IEEE, 2015.
- [19] Dorian Pustina, H Branch Coslett, Peter E Turkeltaub, Nicholas Tustison, Myrna F Schwartz, and Brian Avants. Automated segmentation of chronic stroke lesions using linda: Lesion identification with neighborhood data analysis. *Human brain mapping*, 37(4):1405–1421, 2016.
- [20] Jesper D Nielsen, Kristoffer H Madsen, Oula Puonti, Hartwig R Siebner, Christian Bauer, Camilla Gøbel Madsen, Guilherme B Saturnino, and Axel Thielscher. Automatic skull segmentation from mr images for realistic volume conductor models of the head: Assessment of the state-of-the-art. *Neuroimage*, 174:587–598, 2018.
- [21] Victoria Montes-Restrepo, Pieter van Mierlo, Gregor Strobbe, Steven Staelens, Stefaan Vandenberghe, and Hans Hallez. Influence of skull modeling approaches on eeg source localization. *Brain topography*, 27(1): 95–111, 2014.
- [22] Guilherme B Saturnino, Oula Puonti, Jesper D Nielsen, Daria Antonenko, Kristoffer Hougaard H Madsen, and Axel Thielscher. Simnibs 2.1: A comprehensive pipeline for individualized electric field modelling for transcranial brain stimulation. *bioRxiv*, page 500314, 2018.
- [23] Tonya L Rich and Bernadette T Gillick. Electrode placement in transcranial direct current stimulation-how reliable is the determination of c3/c4? *Brain sciences*, 9(3):69, 2019.
- [24] ALHMW van Lier, A Kolk, Manon Brundel, J Hendriske, J Luijten, J Lagendijk, and C van den Berg. Electrical conductivity in ischemic stroke at 7.0 tesla: a case study. In *Proceedings of the 20th Scientific Meeting of the International Society of Magnetic Resonance in Medicine (ISMRM12)*, volume 3484, 2012.
- [25] Thomas Cattagni, Maxime Geiger, Anthony Supiot, Philippe de Mazancourt, Didier Pradon, Raphael Zory, and Nicolas Roche. A single session of anodal transcranial direct current stimulation applied over the affected primary motor cortex does not alter gait parameters in chronic stroke survivors. *Neurophysiologie Clinique*, 2019.
- [26] Bernhard Elsner, Gert Kwakkel, Joachim Kugler, and Jan Mehrholz. Transcranial direct current stimulation (tdcs) for improving capacity in activities and arm function after stroke: a network meta-analysis of randomised controlled trials. *Journal of neuroengineering and rehabilitation*, 14(1):95, 2017.
- [27] Manuela Hamoudi, Heidi M Schambra, Brita Fritsch, Annika Schoechlin-Marx, Cornelius Weiller, Leonardo G Cohen, and Janine Reis. Transcranial direct current stimulation enhances motor skill learning but not generalization in chronic stroke. *Neurorehabilitation and neural repair*, 32(4-5):295–308, 2018.
- [28] Sumientra M Rampersad, Dick F Stegeman, and Thom F Oostendorp. Single-layer skull approximations perform well in transcranial direct current stimulation modeling. *IEEE Transactions on Neural Systems and Rehabilitation Engineering*, 21(3):346–353, 2012.
- [29] David B Fischer, Peter J Fried, Giulio Ruffini, Oscar Ripolles, Ricardo Salvador, J Banus, WT Ketchabaw, Emiliano Santarnecchi, Alvaro Pascual-Leone, and Michael D Fox. Multifocal tdcs targeting the resting state motor network increases cortical excitability beyond traditional tdcs targeting unilateral motor cortex. *Neuroimage*, 157:34–44, 2017.
- [30] Anna Fertoni, Clarissa Ferrari, and Carlo Miniussi. What do you feel if i apply transcranial electric stimulation? safety, sensations and secondary induced effects. *Clinical Neurophysiology*, 126(11):2181–2188, 2015.
- [31] Tim Wagner, Felipe Fregni, Shirley Fecteau, Alan Grodzinsky, Markus Zahn, and Alvaro Pascual-Leone. Transcranial direct current stimulation: a computer-based human model study. *Neuroimage*, 35(3):1113–1124, 2007.
- [32] Kaori L Ito, Hosung Kim, and Sook-Lei Liew. A comparison of automated lesion segmentation approaches for chronic stroke t1-weighted mri data. *bioRxiv*, page 441451, 2018.

VI. APPENDIX

A. SEGMENTATION BY LINDA

All information of Appendix A. is retrieved from the paper of Pustina et al. (2016)[19] and the review of Ito et al. (2018) [32]

A mono channel algorithm makes use of a single volume, LINDA uses a T1w. Phenomena belonging to chronic stroke lesions, such as cortical necrosis, are visible on T1w, which makes the volume suitable as an input. By identifying the lesion, not only the signal in the voxel itself is taken into account by LINDA but also 26 neighbouring voxels. This is required because the segmentation is dependent on the surrounding context. An example is that white matter hyperintensities should be labelled as lesion only if they extend from the core ischemic zone.

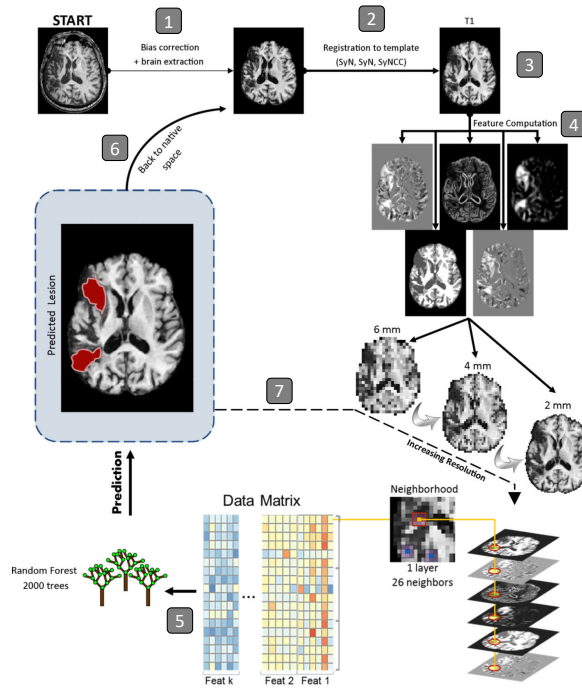


Fig. 6. Workflow of LINDA[19]

The workflow of the LINDA algorithm will be explained step wise.

- 1) Firstly, the data will be preprocessed with two iterations of bias correction and brain extraction and spatial normalisation was performed.
- 2) Then the T1w is registered from native to template space to require the elimination of the lesion from computations to avoid unrealistic deformations. It is also necessary that some features are computed as deviations from the template. The template is built from 208 elderly subjects, where 115 healthy controls and 93 patients with various diseases were included.
- 3) The first registration of the lesion mask is exposed by flipping the T1w in the y-axis and subtract it from each other.
- 4) Six features were computed from the T1w; 1) deviation of k-mean segmentation from controls, 2) gradient magnitude, 3) T1w deviation from controls, 4) k-mean segmentation, 5) deviation of T1w asymmetry from controls, and 6) raw T1w volume.
- 5) These features were fed to the Random Forest (RF) classifier. A set of 60 T1w trained this classifier. A matrix containing data from all subjects is used to train the RF model. Each row of the matrix contains information about a single voxel of a single subject and includes values from neighbouring voxels on all features as columns. Thus the model is trained to classify voxels based not only on the value of the voxel itself but also on its neighbours. The status of the voxel (e.g., 1=healthy, 2=lesion) is used as ground truth outcome to train the RFs which were manually classified in advanced. With this classifier, a posterior probability of healthy tissue or posterior probability of lesion is assigned to a voxel. In the first round, this is done on a resolution of 6mm. By the next round, the posterior probabilities of healthy or lesion tissue are used as an additional feature.
- 6) The predicted lesion mask is registered from template space back to native space to improve detection accuracy.

- 7) Three hierarchical cycles were fulfilled with downsampling resolution of 6mm, 4mm, and 2mm. For the three different resolutions, the neighbourhood radius was 26 voxels, so for the lowest resolution, the voxels are larger; consequently, the neighbourhood information is wider.
- 8) At the highest resolution, posterior probabilities are converted into a discrete segmentation map. The voxel is classified according to the highest posterior probability. For example, a voxel with 60% healthy and 40% lesioned is classified as healthy.
- 9) For right hemisphere lesions, the T1w is flipped back.

A. Model assumptions of LINDA

Before working with LINDA, a few model assumptions should be taken into account. The algorithm is trained for chronic left-sided stroke lesions. So before starting, the T1w should be visualised to see if the stroke patient has a left-hemispheric lesion. If not, the T1w should be mirrored. Chronic is assumed to be between 3 to 154 months post stroke. Moreover, the automatic algorithm is created and tested to predict a specific lesion type, the stroke lesion. Therefore the accuracy of the method outside of the domain it was created for is typically scarce. Another assumption is that the manually segmented lesions are considered correct. Based on a single expert who either drew the lesions (approximately two-thirds) or reviewed the tracings completed by individuals he had trained. In addition to these model assumptions, the lesion size and location should be taken into account. LINDA was biased to recognise larger lesions and cortical ones. Due to the subcortical, brainstem and cerebellar strokes occur less frequently and are often smaller than cortical lesions.

B. RESULTS ELECTRIC FIELD STRENGTH TARGET AREA

TABLE IV
QUANTITATIVE RESULTS OF SIMULATING 2MA TDCS IN TARGET AREA

σ_l [S/m]	Stimulation of the ipsilesional Motor Cortex					Stimulation of the contralesional Motor Cortex				
	E_{mx}^{MC} [V/m]	E_{mn}^{MC} [V/m]	ΔE_{mn}^{MC} Model 1	E_{mn}^L [V/m]	E_{mx}^L [V/m]	E_{mx}^{MC} [V/m]	E_{mn}^{MC} [V/m]	ΔE_{mn}^{MC} Model 1	E_{mn}^L [V/m]	E_{mx}^L [V/m]
0.50	0.51814	0.42680	63.07%	0.29016	16.318	0.52913	0.30571	-1.356%	0.13819	1.0042
0.65	0.49201	0.39696	51.66%	0.25159	16.159	0.52968	0.30714	-0.8935%	0.12520	0.98071
0.80	0.46429	0.37261	42.36%	0.22314	15.968	0.53016	0.30835	-0.5010%	0.11488	0.95131
0.95	0.44663	0.35221	34.57%	0.20108	15.770	0.53060	0.30941	-0.1617%	0.10640	0.92014
1.10	0.43672	0.33477	27.90%	0.18339	15.574	0.53099	0.31033	0.1357%	0.099250	0.88904
1.25	0.42710	0.31964	22.12%	0.16882	15.385	0.53135	0.31114	0.3994%	0.093117	0.85886
1.40	0.41770	0.30637	17.05%	0.15658	15.204	0.53168	0.31188	0.6351%	0.087778	0.82997
1.55	0.40863	0.29460	12.56%	0.14612	15.031	0.53198	0.31253	0.8576%	0.083076	0.80252
1.70	0.39994	0.28409	8.54%	0.13707	14.867	0.53226	0.31313	1.040%	0.078896	0.77653
1.85	0.39166	0.27463	4.91%	0.12914	14.710	0.53251	0.31368	1.216%	0.075150	0.75197
2.00	0.38377	0.26607	1.66%	0.12214	14.562	0.53276	0.31417	1.377%	0.071770	0.72877

From left to right: Conductivity value assigned to lesion (σ_l), Maximum electric field strength in motor cortex (E_{mx}^{MC}), Mean electric field strength in motor cortex (E_{mn}^{MC}), Difference of mean electric field strength in Model 2 compared to Model 1 (ΔE_{mn}^{MC}), Mean electric field strength in lesion (E_{mn}^L), Maximum electric field strength in lesion (E_{mx}^L).

C. ELECTRIC FIELD STRENGTH DISTRIBUTION IN TARGET AREA

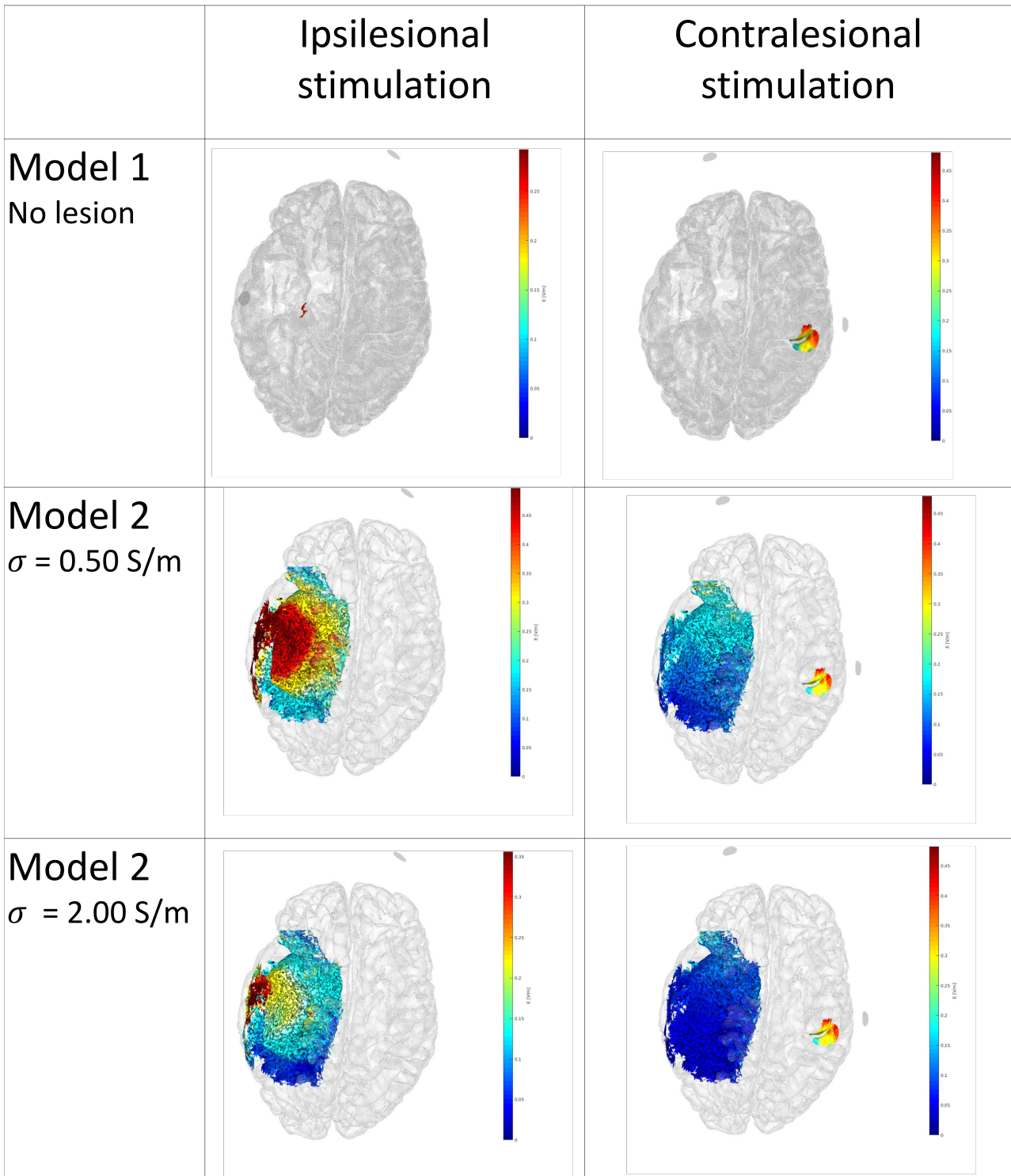


Fig. 7. Electric field strength in the motor cortex and the lesion with tDCS simulation of the ipsilesional motor cortex

D. MATLAB CODE

```

1  %% TOTAL script
2  % Creates a Volume Conduction Model for chronic stroke patients
3  % Compares the developed volume conduction model with outcomes of SimNIBS
4
5  % Requirements pipeline:
6  %   SimNIBS 2.1.2 (including: SPM12 and CAT12)
7  %   LINDA version 0.5.0
8  %   Fieldtrip
9  %   R version 3.5.3 (2019-03-11)
10 %   Add SimNIBS and Fieldtrip to the Matlab path
11 %   Replace the \simnibs_2.1.2\matlab\functions\standard_cond.m matlab function of SimNIBS
12
13 % USAGE:
14 %   LesionConductivity: Lesion conductivity values
15 %   cond_lesion: Lesion conductivity value without decimals
16 %   To run segmentations uncomment line 31 (commented due to time
17 %   consuming process)
18 %   To run simulations uncomment line 135 and line 151 (commented due to time
19 %   consuming process)
20
21 clear all;
22 close all;
23 clc;
24 %% Segmentation whole head
25 % SimNIBS
26 c = sprintf('cd Data/401 ; headreco all --cat 401 401_T1_L.nii -d no-conform');
27 % all = all reconstructions steps,
28 % 401 = name output folder,
29 % 401_T1_L.nii = MRI data
30 % -d no-conform = to keep the axis of the MRI (Saturnino et
31 %   al., 2018)
32 %system(c); % Call SimNIBS from the terminal
33
34 % Load Segmented Data
35 % Segmentation mesh by SimNIBS
36 m1_seg = mesh_load_gmsh4([pwd, filesep, 'Data/401/401_5.msh']); % load mesh segmented by SimNIBS
37 % into scalp, skull, GM, WM and CSF
38 m2_seg = mesh_load_gmsh4([pwd, filesep, 'Data/401/401_5.msh']); % load mesh segmented by SimNIBS
39 % into scalp, skull, GM, WM, CSF and lesion
40 %% Segmentation lesion
41 % LINDA
42 % Load Lesion mask segmented by LINDA:
43 lesion = ft_read_mri('Data/401/linda/Prediction3_native.nii.gz'); % load lesion mask
44 %% Creating a mesh
45
46 % 1. Find coordinates of lesion mask
47 [r,c,v] = ind2sub(size(lesion.anatomy),find(lesion.anatomy == 1)); % Coordinates lesion voxels
48 lesion_vox = [r c v]; % voxels of the lesion
49 sc = lesion_vox*lesion.transform(1:3,1:3);
50 lesion_coordinates = sc + repmat(lesion.transform(1:3,4)', size(sc,1),1); % coordintes of lesion
51 % center
52 wx = 1; wy = 0.9375; wz = wy; % voxel dimensions
53
54 % 2. Find centers of elements:
55 centers_triangles = mesh_get_triangle_centers(m2_seg); % Centers triangles
56 centers_tetrahedron = mesh_get_tetrahedron_centers(m2_seg); % Centers tetrahedrons
57
58 % Filter on distance between voxel and element
59 % tetrahedrons
60 [idx_vox_tet,D] = knnsearch(lesion_coordinates,centers_tetrahedron); %index voxel closest to element
61 % , D = distance between element and closest voxel
62 A_tet = [idx_vox_tet, D];
63 A_tet(:,3) = 1:size(A_tet,1); %element index
64 A_tet(A_tet(:,2)>2,:) = []; % Only keep indeces with a distance shorter than 2mm
65
66 % Triangles
67 [idx_vox_tri,D] = knnsearch(lesion_coordinates,centers_triangles); %index voxel closest to element,
68 % D = distance between element and closest voxel
69 A_tri = [idx_vox_tri, D];
70 A_tri(:,3) = 1:size(A_tri,1); %element index
71 A_tri(A_tri(:,2)>2,:) = []; % Only keep indeces with a distance shorter than 2mm
72
73 % 3. Find elements within lesion voxels
74 % tetrahedrons
75 for i = 1:length(A_tet);
76     if centers_tetrahedron((A_tet(i,3)),1) > lesion_coordinates(A_tet(i,1),1) - wx/2 &&
77         centers_tetrahedron((A_tet(i,3)),1) < lesion_coordinates(A_tet(i,1),1) + wx/2 && ...

```

```

73         centers_tetrahedron((A_tet(i,3)),2) > lesion_coordinates(A_tet(i,1),2) - wy/2 &&
           centers_tetrahedron((A_tet(i,3)),2) < lesion_coordinates(A_tet(i,1),2) + wy/2 && ...
74         centers_tetrahedron((A_tet(i,3)),3) > lesion_coordinates(A_tet(i,1),3) - wz/2 &&
           centers_tetrahedron((A_tet(i,3)),3) < lesion_coordinates(A_tet(i,1),3) + wz/2
75         K_tet(i,1) = A_tet(i,3); % gives indices of lesion elements
76     end
77 end
78 K_tet(K_tet==0) = []; % delete zero's
79
80 % Triangles
81 for i = 1:length(A_tri);
82     if centers_triangles((A_tri(i,3)),1) > lesion_coordinates(A_tri(i,1),1) - wx/2 &&
           centers_triangles((A_tri(i,3)),1) < lesion_coordinates(A_tri(i,1),1) + wx/2 && ...
83         centers_triangles((A_tri(i,3)),2) > lesion_coordinates(A_tri(i,1),2) - wy/2 &&
           centers_triangles((A_tri(i,3)),2) < lesion_coordinates(A_tri(i,1),2) + wy/2 && ...
84         centers_triangles((A_tri(i,3)),3) > lesion_coordinates(A_tri(i,1),3) - wz/2 &&
           centers_triangles((A_tri(i,3)),3) < lesion_coordinates(A_tri(i,1),3) + wz/2
85         K_tri(i,1) = A_tri(i,3); % gives indices of lesion elements
86     end
87 end
88 K_tri(K_tri==0) = []; % delete zero's
89
90 % 4. Replace corresponding labels with lesion label (10)
91 m2_seg.triangle_regions(K_tri)=1010;
92 m2_seg.tetrahedron_regions(K_tet)=10;
93
94 % Save modified mesh of Model 2
95 mesh_save_gmsh4(m2_seg, 'Data/401/401_6');
96
97 %% Electrode configuration
98 % Electrode configuration 1 (stimulate left MC)
99 configuration(1).e1 = 'C3'; % Location eletrode 1
100 configuration(1).e2 = 'Fp2'; % Location eletrode 2
101
102 % Electrode configuration 2 (stimulate right MC)
103 configuration(2).e1='C4'; % Location eletrode 1
104 configuration(2).e2='Fp1'; % Location eletrode 2
105
106 % General stimulation settings
107 S = sim_struct('SESSION');
108 S.poslist{1} = sim_struct('TDCSLIST');
109 S.poslist{1}.currents = [0.002, -0.002]; % Current flow through each channel (mA)
110
111 % First Electrode
112 S.poslist{1}.electrode(1).channelnr = 1; % Connect the electrode to the first channel
113 S.poslist{1}.electrode(1).shape = 'ellipse'; % Elliptical shape
114 S.poslist{1}.electrode(1).dimensions = [10, 10]; % Dimension in mm
115 S.poslist{1}.electrode(1).thickness = 3; % 3 mm thickness
116
117 % Second Electrode
118 S.poslist{1}.electrode(2).channelnr = 2; % Connect the electrode to the second
   channel
119 S.poslist{1}.electrode(2).shape = 'ellipse'; % Elliptical shape
120 S.poslist{1}.electrode(2).dimensions = [10, 10]; % Dimension in mm
121 S.poslist{1}.electrode(2).thickness = 3; % 3 mm thickness
122
123 %% tDCS simulations
124 for j = 1:length(configuration) % For every configuration tDCS simulation
125     S.poslist{1}.electrode(1).centre = configuration(j).e1; % Location electrode 1
126     S.poslist{1}.electrode(2).centre = configuration(j).e2; % Location electrode 2
127     folder_name = ['Data/401/', num2str(configuration(j).e1), '_', num2str(configuration(j).e2),
   '_simulation'];
128     mkdir(folder_name); % Make folder for output
129
130 %% Calculations
131 % Model 1
132 S.fnamehead = 'Data/401/401_5.msh'; % Mesh to simulate stimulation
133 S.pathfem = ['Data/401/', num2str(configuration(j).e1), '_', num2str(configuration(j).e2),
   '_simulation/simulation_5']; % Set path for the simulation output
134
135 % run_simnibs(S) % Run the simulation
136
137 % Load simulation data
138 temp = mesh_load_gmsh4(['Data/401/', num2str(configuration(j).e1), '_', num2str(configuration(j)
   .e2), '_simulation/simulation_5/401_5_TDCS_1_scalar.msh']); % load simulation of
   Model 1
139 temp.max = []; temp.max_index = []; temp.max_perc= [];
140 ml.configuration(j) = temp; clear temp;
141
142 % Model 2

```

```

143     S.fnamehead = 'Data/401/401_6.msh'; % Mesh to simulate
        stimulation
144     cond_lesion = [50 65 80 95 110 125 140 155 170 185 200];
145     LesionConductivity = [0.50 0.65 0.80 0.95 1.10 1.25 1.40 1.55 1.70 1.85 2.00];
146     for i = 1:length(cond_lesion)
147         S.pathfem = sprintf('Data/401/%s_%s_simulation/simulation_6_%d',configuration(j).e1,
            configuration(j).e2, cond_lesion(i)); % Folder for the simulation output %2f',
            cond_lesion(i));
148         S.poslist{1,1}.cond(10).value = LesionConductivity(i); %
            Lesion conductivity
149         S.subpath = 'Data/401/m2m_401_5';
150
151     %         run_simnibs(S) % Run the simulation
152     end
153
154     % Load simulation data
155     for i = 1:length(cond_lesion)
156         m2(j).configuration(i).mesh_name = sprintf('m2_%d', cond_lesion(i));
157         file_name = sprintf('Data/401/%s_%s_simulation/simulation_6_%d/401_6_TDCS_1_scalar.msh',
            configuration(j).e1, configuration(j).e2, cond_lesion(i));
158         m2(j).configuration(i).output = mesh_load_gmsh4(file_name);
159     end
160
161 %% Analysis – General results
162 % Range E in GM
163 for i = 1:length(cond_lesion)
164     max_E(j).configuration(i)=max(m2(j).configuration(i).output.element_data{2, 1}.tetdata(m2(j).
        configuration(i).output.tetrahedron_regions==2));
165     min_E(j).configuration(i)=min(m2(j).configuration(i).output.element_data{2, 1}.tetdata(m2(j)
        .configuration(i).output.tetrahedron_regions==2));
166 end
167 max_E_tot(j)=max(max_E(j).configuration)
168 min_E_tot(j)=min(min_E(j).configuration);
169 %% Result Analysis – Whole GM Volume
170 % Max E in GM of Model 1
171 m1.configuration(j).max = max(m1.configuration(j).element_data{2, 1}.tetdata(m1.configuration(j).
    tetrahedron_regions==2)); % max E
172 m1.configuration(j).max_index = find(m1.configuration(j).element_data{2, 1}.tetdata==m1.
    configuration(j).max); % Index of max E
173 % Max E in GM of Model 2
174 for i = 1:length(LesionConductivity)
175     m2(j).configuration(i).max = max(m2(j).configuration(i).output.element_data{2, 1}.tetdata(m2(j).
        configuration(i).output.tetrahedron_regions==2)); % max E
176     m2(j).configuration(i).max_index = find(m2(j).configuration(i).output.element_data{2, 1}.tetdata
        ==m2(j).configuration(i).max); % Index of max E
177     m2(j).configuration(i).max_perc = (m2(j).configuration(i).max - m1.configuration(j).max) ./m1.
        configuration(j).max*100;
178 end
179
180 %% Analysis – Target area
181 %% Find Motor Cortex (MC)
182 %     mesh_show_surface(m2(j).configuration(1).output); end % Shows only gray matter
183 %
184 % % Click on motor cortex
185 %     dcm_obj(j) = datacursormode(gcf);
186 %     k = 0;
187 %     while k == 0
188 %         set(dcm_obj(j), 'DisplayStyle', 'window', 'SnapToDataVertex', 'on', 'Enable', 'on');
189 %         k = waitforbuttonpress;
190 %     end
191 %     c_info.configuration(j) = getCursorInfo(dcm_obj(j));
192 %     MC_center(j).configuration = c_info.configuration(j).Position; % coordinates of center of
    sphere of MC
193 %% Pointed by Medical Doctor
194 MC_center(1).configuration = [-19.095 21.61 33.0]; % Ipsilesional motor cortex
195 MC_center(2).configuration = [50.02 3.593 19.85]; % Contralesional motor cortex
196
197 % Make sphere representing the target area MC
198 r =10; % radius in mm of sphere
199
200 % Find index triangles of sphere
201 D_MC_tri = pdist2(centers_triangles,MC_center(j).configuration, 'euclidean'); %Distance between
    all tetrahedron centers and center of MC
202 D_MC_tri(:,2) = 1:size(D_MC_tri,1); % Add tetrahedron index
203 D_MC_tri(D_MC_tri(:,1)>r,:) = []; % Only keep indeces of tetrahedrons with a distance shorter
    than 10mm, so it is in the sphere
204 for ii=1:length(D_MC_tri)
205     if m2(j).configuration(1).output.triangle_regions(D_MC_tri(ii,2))==1002 % Only de GM within
        the sphere
206         MC_tri_index(j).configuration(ii,1) = D_MC_tri(ii,2);

```

```

207     end
208 end
209 MC_tri_index(j).configuration(MC_tri_index(j).configuration==0) = []; %delete zero`s
210
211 % Find index tetrahedrons of sphere
212 D_MC_tet = pdist2(centers_tetrahedron,MC_center(j).configuration,'euclidean'); %Distance between
    all tetrahedron centers and center of MC
213 D_MC_tet(:,2) = 1:size(D_MC_tet,1); % Add tetrahedron index
214 D_MC_tet(D_MC_tet(:,1)>r,:) = []; % Only keep indeces of tetrahedrons with a distance shorter
    than 10mm, so it is in the sphere
215 for ii=1:length(D_MC_tet)
216     if m2(j).configuration(1).output.tetrahedron_regions(D_MC_tet(ii,2))==2 % Only de GM within
        the sphere
217         MC_tet_index(j).configuration(ii,1) = D_MC_tet(ii,2);
218     end
219 end
220 MC_tet_index(j).configuration(MC_tet_index(j).configuration==0) = []; %delete zero`s
221
222 % Calculate mean and max E of the tetrahedrons in MC and in lesion
223 % Model 1:
224 MC_meanE_m1(j).configuration = mean(m1.configuration(j).element_data{2,1}.tetdata(MC_tet_index(
    j).configuration));
225 MC_maxE_m1(j).configuration = max(m1.configuration(j).element_data{2,1}.tetdata(MC_tet_index(j)
    .configuration));
226
227 % Model 2:
228 for i=1:length(cond_lesion)
229     % Motor Cortex
230     MC_meanE_m2(j).configuration(i) = mean(m2(j).configuration(i).output.element_data{2,1}.
        tetdata(MC_tet_index(j).configuration));
231     m2(j).configuration(i).MC_maxE = max(m2(j).configuration(i).output.element_data{2,1}.
        tetdata(MC_tet_index(j).configuration));
232     % Lesion
233     lesion_tet_index(j).configuration=find(m2(j).configuration(i).output.element_data{2,1}.
        tetdata(m2(j).configuration(i).output.tetrahedron_regions==10));
234
235     m2(j).configuration(i).lesion_meanE = mean(m2(j).configuration(i).output.element_data{2,1}.
        tetdata(K_tet));
236     m2(j).configuration(i).lesion_maxE = max(m2(j).configuration(i).output.element_data{2,1}.
        tetdata(K_tet));
237
238     % Percentage difference of mean E (M2-M1./M1*100)
239     m2(j).configuration(i).MC_dif=(MC_meanE_m2(j).configuration(i) - MC_meanE_m1(j).
        configuration) ./ MC_meanE_m1(j).configuration * 100;
240 end
241 end
242 %%% FIGURES
243 %%% Fig. 3
244 % M1 Ipsilesional Stimulation
245 figure(1);
246 j=1;
247 mesh_show_surface(m1.configuration(j),'colormap',jet,'showElec',false,'scaleLimits',[0 max_E(1).
    configuration(end)]);
248 title('Model 1 Ipsilesional Stimulation');
249
250 % M1 Contralesional Stimulation
251 figure(2);
252 j=2;
253 mesh_show_surface(m1.configuration(j),'colormap',jet,'showElec',false);
254 title('Model 1 Contralesional Stimulation');
255
256 % M2 Ipsilesional Stimulation with lesion conductivity of 0.50 S/m
257 figure(3);
258 j=1;
259 i=1;
260 mesh_show_surface(m2(j).configuration(i).output,'colormap',jet,'showElec',false);
261 title(['Model 2 Ipsilesional Stimulation with lesion conductivity of ', num2str(LesionConductivity(i))
    , ' [S/m]']); %Electric field strength, through GM
262
263 % M2 Contralesional Stimulation with lesion conductivity of 0.50 S/m
264 figure(4);
265 j=2;
266 i=1;
267 mesh_show_surface(m2(j).configuration(i).output,'colormap',jet,'showElec',false);
268 title(['Model 2 Contralesion Stimulation with lesion conductivity of ', num2str(LesionConductivity(i)
    )), ' [S/m]']);
269
270 % M2 Ipsilesional Stimulation with lesion conductivity of 2.00 S/m
271 figure(5);
272 j=1;

```

```

273 i=length(LesionConductivity);
274 mesh_show_surface(m2(j).configuration(i).output, 'colormap', jet, 'showElec', false);
275 title(['Model 2 Ipsilesion Stimulation with lesion conductivity of ', num2str(LesionConductivity(i))
, ' [S/m]']);
276
277 % M2 Contralesional Stimulation with lesion conductivity of 2.00 S/m
278 figure(6);
279 j=2;
280 i=length(LesionConductivity);
281 mesh_show_surface(m2(j).configuration(i).output, 'colormap', jet, 'showElec', false);
282 title(['Model 2 Contralesion Stimulation with lesion conductivity of ', num2str(LesionConductivity(i)
)), ' [S/m]']);
283 %% Fig. 4 Visualization of the GM and the target areas
284 tet_centers_lesion = centers_tetrahedron(K_tet,:); % Lesion
285 tet_centers_MC_L = centers_tetrahedron(MC_tet_index(1).configuration,:); % Ipsilesional motor cortex
286 tet_centers_MC_R = centers_tetrahedron(MC_tet_index(2).configuration,:); % contralesional motor
cortex
287 centers_tetrahedron_m2(2).configuration = mesh_get_tetrahedron_centers(m2(2).configuration(1).output
);
288 centers_tetrahedron_GM(2).configuration = centers_tetrahedron_m2(2).configuration(m2(2).
configuration(1).output.tetrahedron_regions ==2,:);
289 tet_centers_GM = centers_tetrahedron_GM(2).configuration; % GM
290
291 figure(7);
292 a = pointCloud(tet_centers_GM);
293 cmatrix = ones(size(a.Location)).*[0.9 0.9 0.9];
294 a = pointCloud(tet_centers_GM, 'Color', cmatrix);
295 pshow(a)
296 title('Visualization of the GM and the target areas');
297 hold on
298 scatter3( tet_centers_lesion(:,1), tet_centers_lesion(:,2), tet_centers_lesion(:,3)); % Lesion
299 hold on
300 scatter3( tet_centers_MC_L(:,1), tet_centers_MC_L(:,2), tet_centers_MC_L(:,3), 'r'); % Ipsilesional motor
cortex
301 hold on
302 scatter3( tet_centers_MC_R(:,1), tet_centers_MC_R(:,2), tet_centers_MC_R(:,3), 'r'); % contralesional
motor cortex
303 hold on
304 trisurf(m2(j).configuration(i).output.triangles(m2(j).configuration(i).output.triangle_regions
==1002,:), m2(j).configuration(i).output.nodes(:,1), m2(j).configuration(i).output.nodes(:,2), m2(j)
).configuration(i).output.nodes(:,3), ones(size(m2(j).configuration(i).output.nodes(:,3))), '
Facecolor', [192/255 192/255 192/255], 'FaceAlpha', 0.25, 'EdgeAlpha', 0.01) );
305 axis off
306
307 %% Fig. 5 Electric field strength in motor cortex
308 % Ipsilesional Stimulation
309 figure(8);
310 j=1;
311 plot( [min(LesionConductivity), max(LesionConductivity)], [MC_meanE_m1(j).configuration, MC_meanE_m1(j)
).configuration, 'color', [0 0.4470 0.7410], 'linewidth', 3); % straight line for the mean E in
mc in Model 1
312 title('Electric field strength in motor cortex'); xlabel('Lesion conductivity [S/m]'); ylabel('Mean
electric field strength [V/mm]');
313 hold on
314 plot(LesionConductivity, MC_meanE_m2(j).configuration, '.', 'MarkerSize', 40, 'color', [0 0.4470
0.7410] );
315 set(gca, 'FontSize', 32);
316 xticks(LesionConductivity)
317 for i = 1:length(cond_lesion);
318 xt(i) = LesionConductivity(1,i);
319 yt(i) = MC_meanE_m2(j).configuration(1,i);
320 str = [ ' ', num2str(round(m2(j).configuration(i).MC_dif,1)), '%'];
321 text(xt(i), yt(i), str, 'FontSize', 24)
322 end
323
324 % Contralesional Stimulation
325 hold on
326 j=2;
327 plot( [min(LesionConductivity), max(LesionConductivity)], [MC_meanE_m1(j).configuration, MC_meanE_m1(j)
).configuration, 'color', [0.8500 0.3250 0.0980], 'linewidth', 3); % straight line for the mean
E in mc in Model 1
328 title('Electric field strength in motor cortex'); xlabel('Lesion conductivity [S/m]'); ylabel('Mean
electric field strength [V/m]');
329 hold on
330 plot(LesionConductivity, MC_meanE_m2(j).configuration, '.', 'MarkerSize', 40, 'color', [0.8500 0.3250
0.0980]);
331 set(gca, 'FontSize', 32);
332 legend({'Ipsilesional: Model 1'}, 'Model 2', {'Contralesional: Model 1'}, 'Model 2', 'Location', 'best
'})
333 xticks(LesionConductivity)

```

```

334     for i = 1:length(cond_lesion)
335         xt(i) = LesionConductivity(1,i);
336         yt(i)= MC_meanE_m2(j).configuration(1,i);
337         str= [ ' ', num2str(round(m2(j).configuration(i).MC_dif,1)), '%'];
338         text(xt(i),yt(i),str, 'FontSize', 14)
339     end
340
341 %% Fig. 7
342 for j=1:2
343     for i = 1:length(cond_lesion)
344         m2(j).configuration(i).output.triangle_regions(MC_tri_index(j).configuration)=1011;
345         m2(j).configuration(i).output.tetrahedron_regions(MC_tet_index(j).configuration)=11;
346     end
347 end
348 % Model 1 Ipsi
349 figure(9);
350 j=1;
351 m1.configuration(j).triangle_regions(MC_tri_index(j).configuration)=1011;
352 m1.configuration(j).tetrahedron_regions(MC_tet_index(j).configuration)=11;
353 mesh_show_surface(m1.configuration(j),'region_idx',1011, 'colormap', jet);
354 trisurf(m2(j).configuration(i).output.triangles(m2(j).configuration(i).output.triangle_regions
    ==1002,:),m2(j).configuration(i).output.nodes(:,1),m2(j).configuration(i).output.nodes(:,2),m2(j)
    ).configuration(i).output.nodes(:,3),ones(size(m2(j).configuration(i).output.nodes(:,3))),'
    Facecolor',[192/255 192/255 192/255], 'FaceAlpha', 0.25,'EdgeAlpha', 0.01) ;
355 title('Model 1 Ipsilesional stimulation');
356
357 % Model 1 Contra
358 figure(10);
359 j=2;
360 m1.configuration(j).triangle_regions(MC_tri_index(j).configuration)=1011;
361 m1.configuration(j).tetrahedron_regions(MC_tet_index(j).configuration)=11;
362 mesh_show_surface(m1.configuration(j),'region_idx',1011, 'colormap', jet);
363 trisurf(m2(j).configuration(i).output.triangles(m2(j).configuration(i).output.triangle_regions
    ==1002,:),m2(j).configuration(i).output.nodes(:,1),m2(j).configuration(i).output.nodes(:,2),m2(j)
    ).configuration(i).output.nodes(:,3),ones(size(m2(j).configuration(i).output.nodes(:,3))),'
    Facecolor',[192/255 192/255 192/255], 'FaceAlpha', 0.25,'EdgeAlpha', 0.01) ;
364 title('Model 1 Contralesional stimulation');
365
366 % Model 2 Ipsi with lesion conductivity of 0.50 S/m
367 figure(11);
368 j=1;
369 i=1;
370 mesh_show_surface(m2(j).configuration(i).output,'region_idx',1010, 'colormap', jet); %lesion
371 trisurf(m2(j).configuration(i).output.triangles(m2(j).configuration(i).output.triangle_regions
    ==1002,:),m2(j).configuration(i).output.nodes(:,1),m2(j).configuration(i).output.nodes(:,2),m2(j)
    ).configuration(i).output.nodes(:,3),ones(size(m2(j).configuration(i).output.nodes(:,3))),'
    Facecolor',[192/255 192/255 192/255], 'FaceAlpha', 0.25,'EdgeAlpha', 0.01) ;% GM
372 hold on
373 mesh_show_surface(m2(j).configuration(i).output,'region_idx',1011,'colormap', jet);% Motor Cortex
374 title(['Model 2 Ipsilesional stimulation with lesion conductivity ', num2str(LesionConductivity(i))
    ]);
375
376 % Model 2 Contra with lesion conductivity of 0.50 S/m
377 figure(12);
378 j=2;
379 i=1;
380 mesh_show_surface(m2(j).configuration(i).output,'region_idx',1010, 'colormap', jet); %lesion
381 trisurf(m2(j).configuration(i).output.triangles(m2(j).configuration(i).output.triangle_regions
    ==1002,:),m2(j).configuration(i).output.nodes(:,1),m2(j).configuration(i).output.nodes(:,2),m2(j)
    ).configuration(i).output.nodes(:,3),ones(size(m2(j).configuration(i).output.nodes(:,3))),'
    Facecolor',[192/255 192/255 192/255], 'FaceAlpha', 0.25,'EdgeAlpha', 0.01) ;% GM
382 hold on
383 mesh_show_surface(m2(j).configuration(i).output,'region_idx',1011,'colormap', jet);% Motor Cortex
384 title(['Model 2 Contralesional stimulation with lesion conductivity ', num2str(LesionConductivity(i))
    ]);
385
386 % Model 2 Ipsi with lesion conductivity of 2.00 S/m
387 figure(13);
388 j=1;
389 i=LesionConductivity(end);
390 mesh_show_surface(m2(j).configuration(i).output,'region_idx',1010, 'colormap', jet); %lesion
391 trisurf(m2(j).configuration(i).output.triangles(m2(j).configuration(i).output.triangle_regions
    ==1002,:),m2(j).configuration(i).output.nodes(:,1),m2(j).configuration(i).output.nodes(:,2),m2(j)
    ).configuration(i).output.nodes(:,3),ones(size(m2(j).configuration(i).output.nodes(:,3))),'
    Facecolor',[192/255 192/255 192/255], 'FaceAlpha', 0.25,'EdgeAlpha', 0.01) ;% GM
392 hold on
393 mesh_show_surface(m2(j).configuration(i).output,'region_idx',1011,'colormap', jet);% Motor Cortex
394 title(['Model 2 Ipsilesional stimulation with lesion conductivity ', num2str(LesionConductivity(i))
    ]);
395

```

```

396 % Model 2 Contra with lesion conductivity of 2.00 S/m
397 figure(14);
398 j=2;
399 i=LesionConductivity(end);
400 mesh_show_surface(m2(j).configuration(i).output,'region_idx',1010,'colormap',jet);%lesion
401 trisurf(m2(j).configuration(i).output.triangles(m2(j).configuration(i).output.triangle_regions
    ==1002,:),m2(j).configuration(i).output.nodes(:,1),m2(j).configuration(i).output.nodes(:,2),m2(j)
    ).configuration(i).output.nodes(:,3),ones(size(m2(j).configuration(i).output.nodes(:,3))),
    'Facecolor',[192/255 192/255 192/255], 'FaceAlpha', 0.25,'EdgeAlpha', 0.01) );% GM
402 hold on
403 mesh_show_surface(m2(j).configuration(i).output,'region_idx',1011,'colormap',jet);% Motor Cortex
404 title(['Model 2 Contralesional stimulation with lesion conductivity ', num2str(LesionConductivity(i)
    )]);
405
406 %% TABLES
407
408 %% Table II
409 Table2.Total = [length(centers_tetrahedron);length(centers_triangles)];
410 Table2.Lesion =[length(K_tet);length(K_tri)];
411 Table2.MC_i =[length(MC_tet_index(1).configuration);length(MC_tri_index(1).configuration)];
412 Table2.MC_c = [length(MC_tet_index(2).configuration);length(MC_tri_index(2).configuration)];
413 Table2=struct2table(Table2)
414
415 %% Table III
416 % Model 1
417 Table3_M1.Max_E_Ipsi = m1.configuration(1).max;
418 Table3_M1.Max_E_Contra = m1.configuration(2).max;
419 Table3_Model1=struct2table(Table3_M1)
420
421 % Model 2
422 for i = 1:length(LesionConductivity)
423     Table3_M2(i).Lesion_Conductivity = LesionConductivity(i);
424     Table3_M2(i).Max_E_Ipsi = m2(1).configuration(i).max;
425     Table3_M2(i).Max_E_Contra = m2(2).configuration(i).max;
426 end
427 Table3_Model2=struct2table(Table3_M2)
428
429 %% Table IV
430 % Ipsilesional Stimulation
431 j=1;
432 for i = 1:length(LesionConductivity)
433     Table4(i).Lesion_Conductivity = LesionConductivity(i);
434     Table4(i).Max_E_MotorCortex = m2(j).configuration(i).MC_maxE;
435     Table4(i).Mean_E_MotorCortex = MC_meanE_m2(j).configuration(i);
436     Table4(i).Percentage_Dif_Mean_E_MotorCortex = m2(j).configuration(i).MC_dif;
437     Table4(i).Mean_E_Lesion = m2(j).configuration(i).lesion_meanE;
438     Table4(i).Max_E_Lesion =m2(j).configuration(i).lesion_maxE ;
439 end
440     Table4_Ipsilesional=struct2table(T_targetM1(j).configuration)
441
442 % Contralesional Stimulation
443 j=2;
444 for i = 1:length(LesionConductivity)
445     Table4(i).Lesion_Conductivity = LesionConductivity(i);
446     Table4(i).Max_E_MotorCortex = m2(j).configuration(i).MC_maxE;
447     Table4(i).Mean_E_MotorCortex = MC_meanE_m2(j).configuration(i);
448     Table4(i).Percentage_Dif_Mean_E_MotorCortex = m2(j).configuration(i).MC_dif;
449     Table4(i).Mean_E_Lesion = m2(j).configuration(i).lesion_meanE;
450     Table4(i).Max_E_Lesion =m2(j).configuration(i).lesion_maxE ;
451 end
452     Table4_Contralesional=struct2table(T_targetM1(j).configuration)

```